Journal of Marine Biosciences Vol. 1 (1), 50–62, 2015
Print ISSN 2454–3519 Online ISSN 2454–3527

JMBS

Structural Elucidation of *Chlamydia trachomatis* MIP Mutants and Modeling the Interactions with Native Inhibitors

Ramachandran Vijayan[1] and Natesan Manoharan.[*]

[1,*] Department of Marine Science, Bharathidasan University, Trichy – 620 024, India

[*] Corresponding author E. Mail: biomano21@yahoo.com

Abstract

The *Legionella pneumophila*, causes Legionnaires' disease. This human pathogen produces a major virulence factor, called `macrophage infectivity potentiator protein' (Mip), that is essential for multiplication of the bacteria in human alveolar macrophages. Mip exhibits peptidyl prolyl *cis-trans* isomerase (PPIase) activity, which can be inhibited by Rapamycin and FK506. Homologous proteins are *Chlamydia trachomatis* and *Chlamydia pneumoniae*. Chlamydia causes Sexual transmitted disease, Trachoma and Pneumonia. Mutation of Legionella Mip protein on catalytic residues at Aspartate-142 position replaced to Leucine-142 and Tyrosine-185 position replaced to Alanine-185 that strongly reduces the PPIase activity as reported earlier. In order to design a drug for treating *Chlamydia* infections, we aim to design an *in-silico* mutagenesis model of *Chlamydia trachomatis* Mip for both important catalytic residues, validated the stability of the mutated model. Further, we have docked to the known inhibitor rapamycin with *Chlamydia trachomatis* Mip (native) and mutants (D170L and Y213A) to examine the details of conformational changes occurred in the binding site. For electrostatic contributions and VanderWaals interactions are important for rapamycin binding and responsible for the binding differences between the *Chlamydia trachomatis* Mip (native and mutated) proteins. Thus, the observations provide new insights into the structure and function relationship of Mip would be help for designing new marine drugs against Chlamydia pathogens.

Keywords: Chlamydia, Legionella, *in-silico* mutagenesis, rapamycin, molecular docking.

1. INTRODUCTION

Chlamydia are important human that is capable of causing a wide range of diseases [1]. Members of the *Chlamydia* are small obligate intracellular parasites and were formerly believed to be viruses and are true bacteria[2]. *Chlamydia pneumoniae* causes respiratory infections in humans and also pneumonia[3]. *Chlamydia trachomatis* is the most common sexually transmitted bacterial pathogen, with 100 million cases per year worldwide[4]. These pathogens are able to evade the host immune system. *C. trachomatis* Macrophage infectivity potentiator (MIP) is a 27-kDa membrane

protein located in both elementary bodies (EB) and reticulate bodies (RB) [5], with a COOH-terminal region exhibiting peptidyl-prolyl *cis*/*trans* isomerase (PPIase) activity [6]. Homologous proteins are also found in other intra cellular pathogens such *as Legionella pneumophila* MIP [7], *Chlamydia pneumonia [3]* and *Trypnasoma cruzi* [8]. *Legionella* Mip has two domains namely, N and C-terminal. N-terminal is responsible for dimerisation and C-terminal has a 100 residue domain with 35% sequence identity to human FKBP12 [9]. *Legionella* Mip exhibits peptidyl prolyl *cis-trans* isomerase (PPIase) activity which can be inhibited by Rapamycin and FK506 [10]. Rapamycin (sirolimus) is a macrolide produced by the bacterium *Streptomyces hygroscopicus* discovered in the soil of Easter Island. It has immunosuppressive effect in humans and is especially used in kidney transplants. Rapamycin is an oral drug and its bioavailability in a mouse model experiment of metastatic cancer suggests that rapamycin suppress the growth of solid tumors by blocking angiogenesis [11]. The immunosuppressant FK506 (tacrolimus) and rapamycin have similar chemical structures and bind to the same intracellular receptor, FKBP12 (FK506 binding protein). Although, they have different mechanisms of action in cells. The FKBP-FK506 complex inhibits not only the PPIase activity of FKBP and also the phosphatase activity of calcineurin (CaN), thereby preventing the dephosphorylation of Nuclear factor of activated T-cells (NF-AT) that is required for IL-2 gene expression and T-cell activation [12, 13]. Also, rapamycin binds to FKBP12, but the FKBP/rapamycin complex interacts with mammalian target of rapamycin (mTOR) instead of CaN and exerts immunosuppressive activity [14]. Recently reported that mutation of Legionella Mip protein on catalytic residues at Aspartate-142 position replaced to Leucine-142 and Tyrosine-185 position replaced to Alanine-185 which strongly reduces PPIase activity[15]. In order to design a drug to treat chlamydial infections, Therefore we constructed a *in silico* mutagenesis [16] model for both important catalytic residues (Aspartate-170 into Leucine-170) and (Tyrosine-213 into Alanine213) of C. Mip, validated the stability of the mutated model. Further we have docked to the known inhibitor rapamycin with native and mutants of *C. trachomatis* Mip and to analyze the binding affinity. This study will provide a base for designing novel inhibitors for Mip.

2. MATERIALS AND METHODS

2.1 Homology Modeling

The amino acid sequence of *Chlamydia trachomatis* Mip was extracted from the Uniprot Database (accession code:P26623) (http://www.uniprot.org/uniprot/). BLAST (www.ncbi.nlm.nih.gov/blast) search among similar proteins of known 3D structure revealed that the *Legionella pneumophila* Mip had the highest score in the sequence similarity with *Chlamydia species (ssp)* Mip, namely 35% identity. Hence, in this study the X-ray structure of *Legionella pneumophila* Mip (Protein Data Bank code: 1FD9) was selected as a template to predict the 3D structure of *Chlamydia trachomatis* Mip and *Chlamydia pneumoniae* Mip. Sequence alignment was performed with CLUSTALW, using the BLOSUM

matrices [17] for scoring the alignment. Pairwise sequence alignment of the target, *Chlamydia ssp.* with the template, *Legionella pneumophila* Mip, is the crucial step in homology modeling. The obtained alignments were checked for insertions and deletions in the conserved regions manually. The resulting alignment were given as an input for the homology modeling software MODELER [18]. This program assigns the atomic co-ordinates to the regions are structurally aligned with the template, builds intervening loops, and optimizes the rotamers of amino acid side chains, and performs an initial energy optimization of the structure. MODELER [18] generates the protein three-dimensional structures by satisfying the spatial restraints imposed by the sequence alignment with the template. The spatial restraints consist of homology derived restraints on the distances and dihedral angles in the target based on its alignment with the template, stereochemical restraints such as bond length and bond angles from CHARMm force field [19] and the statistical preferences for dihedral angles and non-bonded inter-atomic distances retrieved from a representative set of protein structures. The restraints are expressed in terms of probability density functions (PDF). The three-dimensional homology model of the protein is obtained by probability density function with the target variable target function procedure in the cartesian space that employs methods of conjugate gradients and molecular dynamics with simulated annealing [19]. To achieve sufficient conformational sampling of each active site residue, twenty homology models were generated. Hydrogen atoms were added to the homology models. The homology models were energy minimized with CHARMm force field, in a step-wise manner following a standard procedure consists of 500 steps of steepest descent and 1,000 steps of conjugate gradient with a root mean square (rms) gradient of the potential energy of 0.001kcal/mol Å at each step. The stereo-chemical quality of the final refined model was evaluated using PROCHECK [20].

2.2. Dataset collection:

The protein sequence information for our in-silico analysis was obtained from NCBI database (www.ncbi.nlm.nih.gov). The structure of *C. trachomatis* Mip were obtained from homology modeling. The mutant (D170L and Y213A) structure was built by induced point mutation in the position of 170 and 213 of *C. trachomatis* Mip protein using SPDB viewer package[13]. This structure was energetically optimized by applying the all atom OPLS force field available in SPDB viewer package [21].

2.3.Predicting stability change on mutated single amino acid based on support vector machine (I-Mutant 2.0:

The mutations occurring in the protein coding region may lead to the deleterious consequences and might disturb its 3D structure. Here we I-Mutant 3.0 [22]. Protein structural stability of the mutants were assessed using I-Mutant 2.0 server which is a support vector machine (SVM) based tool for automatic prediction of protein stability changes upon single-point mutations; predictions are performed for both sequence and structure of proteins using I-Mutant 2.0 server[22]. The output of this program shows the predicted free

energy change value (ΔΔG) which is calculated from the unfolding Gibbs free energy value of the native type (kcal/mol). Positive ΔΔG values infers that the mutated protein possesses high stability and vice versa (http://gpcr.biocomp.unibo.it/ cgi/predictors/ I-Mutant 2.0/ I-Mutant 2.0.cgi).

2.4. Structure optimization and validation:

The systems were subjected to optimize the structure by applying the all atom OPLS force field available in SPDB viewer package [21]. Solvent accessibility surface area (SAS) for normal and mutated *C. trachomatis* Mip was calculated using GETAREA [23]. RMSD were carried out by using Structural superimposition by Pymol [24]. No siginificant changes were oberseved in both the mutants (D170L and Y213A) compared to native *C.trachomatis* Mip and the RMSD of 0.05 Å (Fig.1).

2.5. Binding Site Prediction:

To predict the binding site, LIGSITEcsc algorithm [25] and CASTP algorithm [26] were used. LIGSITE[20] which uses connolly surface and defines surface solvent surface events. The algorithm proceeds as follows: the protein is projected onto a 3D grid with a step size of 1.0Å; grid points are labeled as protein, surface, or solvent using certain rules. A grid point is marked as protein if there is at least one atom within 1.6Å. After the solvent excluded surface is calculated the surface vertices coordinates are stored. A sequence of grid points, which starts and ends with surface grid points and which has solvent grid points in between, is called a surface solvent surface event. If the number of surface solvent surface events of a solvent grid exceeds a minimal threshold of 6, then this grid is marked as pocket. Finally, all pocket grid points are clustered according to their spatial proximity. The clusters are ranked by the number of grid points in the cluster[25]. The top three clusters are retained and their centers of mass are used to represent the predicted pocket sites[25]. And also the binding pockets of *C. trachomatis* Mip were identified using CASTP[26] (Computed Atlas of Surface topography of proteins); a program for identifying and characterizing protein active sites, binding sites, and functional residues located on protein surfaces and voids buried in the interior of proteins by measuring concave surface regions on three-dimensional structures of proteins. It also measures the area and volume of pocket or void by solvent accessible surface model (Richards' surface) and by molecular surface model (Connolly's surface). It can also be used to study surface features and functional regions of proteins.

2.6. Molecular Docking studies:

Rapamycin was extracted in the PDB database (http:/www.rcsb.org/pdb) in 2D-strucuture data file (SDF) format were converted into 3D-MOL2 file with the program OpenBABEL2.3.1 [27]. The ligands were further energy minimized for 100 steps with Swiss-PDB viewer with steepest descent and conjugated gradient algorithms [21]. GOLD uses a genetic algorithm to explore the full range of ligand conformational flexibility with partial flexibility of the protein[28]. The Docking was performed using GOLD Software (Genetic Optimization Ligand Docking). GOLD uses a genetic algorithm to explore the full range of ligand

conformational flexibility with partial flexibility of the protein.40 Docking procedure consisted of three interrelated components; a) identification of binding site b) a search algorithm to effectively sample the search space (the set of possible ligand positions and conformations on the protein surface) and c) a scoring function. The GOLD fitness function consisted of four components: a) protein-ligand hydrogen bond energy (external H-bond); b) protein-ligand vanderwals(vdw) energy(external vdw); c) ligand internal vdw energy (internal vdw); d) ligand torsional strain energy(internal torsion). Default settings for GOLD docking were adopted[28]. Ten poses were kept for each ligand, and the one yielding the best score was used. Hydrogen bond interactions of rapamycin with *C. trachomatis* Mip were predicted by Discover Studio[29].

3. RESULTS AND DISCUSSION:

3.1 Protein structure prediction of Chlamydia trachomati Mip

In the absence of crystal structures for *Chlamydia pneumoniae*, homology modeling has been shown to be a valuable tool for gaining insight into the structure and function of the proteins. The pairwise sequence identities of the template of *Legionella pneumopila* Mip (1FD9) with the target, *Chlamydia trachomatis* Mip sequence were relatively low, and their similarity were quite high (50%). Most of the active-site residues were highly conserved. The X-ray crystal structure of the *Legionella pneumophila* Mip provided a better template for the construction of homology models. Based on the template structure of *Legionella* Mip, the homology models of Chlamydia *pneumoniae* Mip was established using MODELER software. The input parameters of the modeling program were set to generate 20 different homology models. Among the 20 models, the ones show the lowest energy, restraint violations, and the conformations of the main chain and side chain were selected for further refinement. The quality of the first model was further improved by energy minimization as described in the materials and methods section(Fig.1). The energy minimizations may help to remove any steric clashes or improper geometries in the protein structure to obtain a model with proper bond angles and bond length.

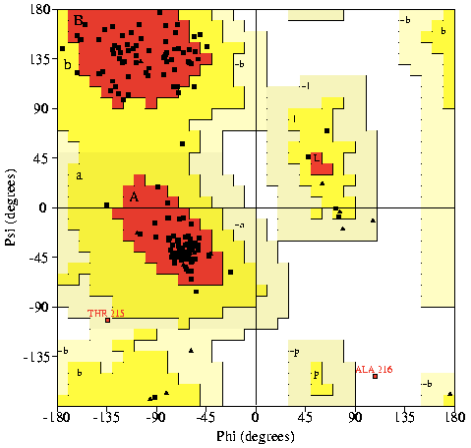

Figure 1: Ramachandran plot of *Chlamydia trachomatis* Mip, the model was validated by Procheck. Red color shows the allowed regions, i.e., right conformation of the amino acid residues. Yellow color regions shows additional allowed regions. White color portion shows the disallowed conformation of the amino acid in the protein structure.

3.2 Protein structure validation:

In order to check the standard of the homology model of *C. trachomatis* Mip

was validated by PROCHECK program. Ramachandran plot show the distribution of the main chain torsion angles, the phi/psi angles of 82.6% residues fell in the most favored regions, 15.2% of the residues lay in the additional allowed regions, and 2.2% residues fell in the generously allowed regions; no residues lay in the disallowed conformations (Fig. 2). The overall conformation of the *Chlamydia trachomatis* Mip model were very similar to the template (Fig.3). Thus, the three-dimensional model of *C. trachomatis* Mip was considered to be accurate.

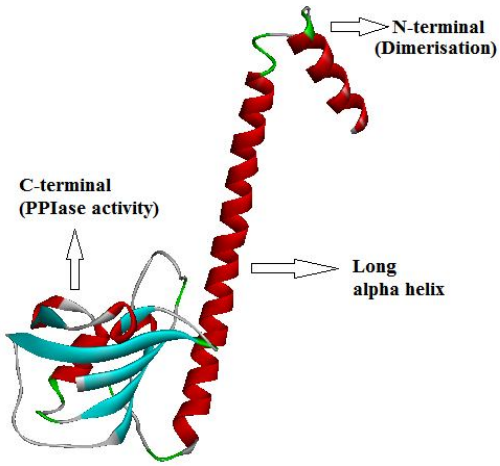

Figure 2: Cartoon representation of *C. trachomatis MIP* showing the two domains (N-terminal domain and C-terminal domain).

3.3. Protein structural stability of the mutants analysis:

In this study, wild type sequence of *C. trachomatis* Mip at 170th position ASP was replaced by LEU to predict protein stability changes through I-mutant server[15]. The results infer loss of stability by the mutant protein with negative Gibbs free energy value of -1.70 at pH 7.0 and 37°C(Table 1). Similarly, wild type sequence of *C. trachomatis* Mip at 213th position TYR was replaced by ALA to predict protein stability changes through I-mutant server. The results show loss of stability by the mutant protein with negative Gibbs free energy value of -1.52 at pH 7.0 and 37°C(Table 1).

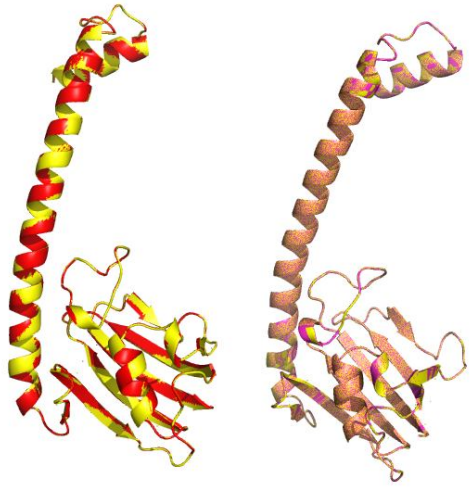

Figure 3: Structural superimposition of native *C. trachomatis* Mip with D170L mutant (left) and superimposition of native *C. trachomatis* Mip with Y213A mutant shows no significant change in the overall structure with an RMSD of 0.07 ºA.

Table 1: Protein structural stability of mutated amino acids of *Chlamydia trachomatis* Mip.

Mutation	Stability	RI	DDG	pH	T
D170L	Decrease	3	-1.70	7.0	37
Y185A	Decrease	8	-1.52	7.0	37

Note: RI: Reliability Index; T: Temperature in Celsius degrees; pH: -log[H+]; DDG: DG(NewProtein)-DG(WildType) in Kcal/mol; DDG<0: Decrease Stability; DDG>0: Increase Stability

3.4. Structure optimization:

Explicit hydrogens were added to the *C. trachomatis* Mip structures of native and Mutant (D170L and Y213A) and was subjected to energy minimization using Swiss-PDB viewer [13] with steepest descent and conjugated gradient algorithms. Energy minimization and relaxation of the loop regions was performed using 300 iterations in a simple minimization method. Again the steepest descent was carried out until the energy showed stability in the sequential repetition.

3.5. Active site analysis of C. trachomatis Mip:

LIGSITE[20] and CASTp[19] programs were used to search the protein binding sites by locating cavities in the *C.trachomatis* Mip structure. Through comparing the conserved residues in family of the studied protein and combining the *inslico* search results, the binding sites of *C.trachomatis* Mip were predicted. Those results were used to guide the following docking experiment. In order to investigate the interaction among *C. trachomatis* Mip with rapamycin, the binding site on the *C. trachomatis* Mip was determined by combining results obtained from LIGSITE [20] and CASTp[19]. All the predictions were found to be synonymous and representing the conserved *Legionella pneumophila* Mip active site residues: Y159, D170, F190, Y213 were correlated with corresponding cavity forming residues in *C.trachomatis* MipY131, D142, W162 and Y185.

3.6. Docking studies of normal and mutants of C. trachomatis Mip with ligands:

The docking studies were performed using the GOLD software [22]. The amino acid residues ASP170 and TYR213 around 5Å were assigned as catalytic region for docking (Fig. 4). The docked complex revealed significant notable features. Calculation of binding energy is very important to understand the affinity level of biological partners. Overall binding energy of the complex mainly contributes to attractive and repulsive van der Waals interaction energy, electrostatic interactions and hydrogen bond (HB) interactions.

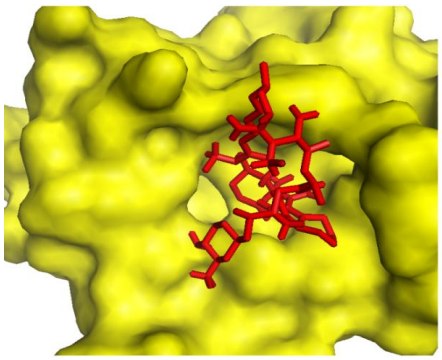

A. Binding pose of C. trachomatis Mip (native) with rapamycin

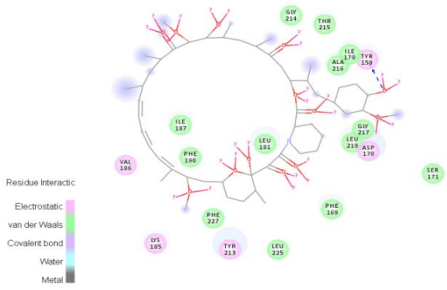

B. Hydrogen bonding interactions for C. trachomatis (native) with rapamycin

Figure 4: Docking confirmation and hydrogen bonding interactions of *C. trachomatis* with Rapamycin (A and B).

Table 2: The binding affinity was calculated by using GOLD score, CHEM score, ASP score and PLP score for normal and mutated *C. trachomatis MIP* and compared with *MIP* inhibitors.

Proteins	**Ligand**	**GOLD score**	**ASP score**
Cht. Mip	Rapamycin	37.17	41.73
D170L Cht. Mip	Rapamycin	34.52	38.96
Y213A Cht. Mip	Rapamycin	30.13	31.70
Cht. Mip	FK506	37.19	42.12
D170L Cht. Mip	FK506	32.57	38.46
Y213A Cht. Mip	FK506	25.68	29.23
Cht. Mip	Cyclosporin	26.31	50.88
D170L Cht. Mip	Cyclosporin	22.72	42.05
Y213A Cht. Mip	Cyclosporin	20.41	47.88

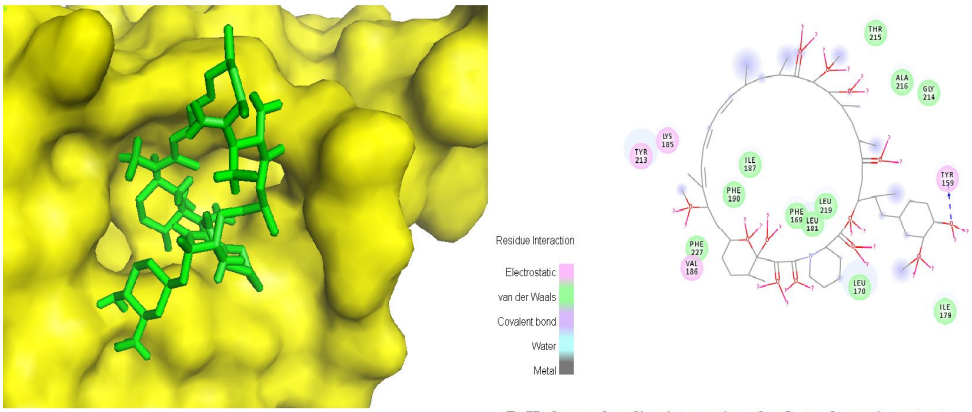

A. Binding pose of C. trachomatis Mip (D170L with rapamycin

B. Hydrogen bonding interactions for C. trachomatis mutant (D170L) with rapamycin

Figure 5: Docking confirmation and hydrogen bonding interactions of *C. trachomatis* mutant (D170L) with Rapamycin (A and B).

The normal *C. trachomatis* Mip has the binding affinity of 37.17 with rapamycin (Table 2) and (Figure 4). The residues Y159 interacted through hydrogen bond with rapamycin (Figure 4). The interaction was found to span within the chosen active site. There are 13 residues forming VanderWaals interactions for native *C. trachomatis* Mip with rapamycin(Figure 4). 5 electrostatic interactions were observed in native *C. trachomatis* Mip-rapamycin complex(Figure 4).

The D170L has the binding affinity of 34.52 with rapamycin (Table 2) and (Figure 5). The results of docking study infer that both the normal and Mutant interact with *C. trachomatis* Mip at the same binding pocket region. However, D170L mutant showed deviation in terms of interaction with *C. trachomatis* Mip by excluding hydrogen bond formation with Y159. 11 residues are forming VanderWaals interactions with D170L mutant-rapamycin complex. (Figure 5). 4 electrostatic interactions were formed in D170L-rapamycin docking (Figure 5).

Solvent Accessibility Surface area (SAS)[17] was calculated for *C. trachomatis* Mip (without mutation) and that after each of such in silico mutation mentioned above (Table 3). Subsequently, we studied the effects of substitution of Asp-170 to Leu-170 on SAS and binding affinities with rapamycin. The results showed that the size of the cavity and binding affinity with rapamycin, were significantly decreased (Table 3). Less binding affinity was observed compared to native *C. trachomatis* Mip-rapamycin. This clearly indicates that the effect of mutation in D170L and the interaction with rapamycin.

Replacement of Tyr-213 to Ala-213 *C. trachomatis* Mip has the binding affinity of 30.13 with rapamycin (Table 2) and (Figure 6). However, Y213A mutant showed that the size of the cavity and binding affinity with rapamycin, were significantly decreased (Table 3). One hydrogen bond interactions were observed with Y213A-rapamycin complex. 10 residues are forming VanderWaals interactions with Y213A mutant-rapamycin complex. (Figure 6). 4 electrostatic interactions were formed in Y213A-rapamycin docking (Figure 6). Less binding affinity was observed compared to native *C. trachomatis* Mip-rapamycin.

The significant conformational changes in binding residues and the interactions are clearly shown (Fig. 4, Fig.5, Fig.6). In D170L and Y213A mutant, the binding residues of Y159, D170, F190, Y213 exhibited more flexibility than native. Due to flexible conformation, in both the mutants showed significant changes in the active site and affects the orientation of the rapamycin binding ((Fig. 4, Fig.5, Fig.6). Docking analysis suggested that D170L and Y213A mutation has strong evidence of less binding affinity compared to the native *C. trachomatis* Mip docking with rapamycin leads to significant changes in the active site and the interactions. And this damage can alter the binding phenomenon between *C. trachomatis* Mip and rapamycin. Our findings support that D170 to L170 mutation and Y213 to A213 substitution resulted in strongly reduced PPIase activity of the recombinant Mip proteins. These results can be further implemented for drug designing process and develop a potent Mip inhibitors for *C. trachomatis* associated diseases.

Table 3: Solvent accessibility surface area (SAS) for normal and mutated *C. trachomatis* Mip.

Protein	**Total (SAS) Å**	**Per Residue (SAS) Å (Normal)**	**Per Residue (SAS) Å (Mutation)**	**% Change**
Cht. Mip (NORMAL)	10885.26			
D170L Cht Mip (MUTATION)	10850.32	59.09	33.70	42.9
Y213A Cht. Mip(MUTATION)	10852.14	109.32	50.07	54.2

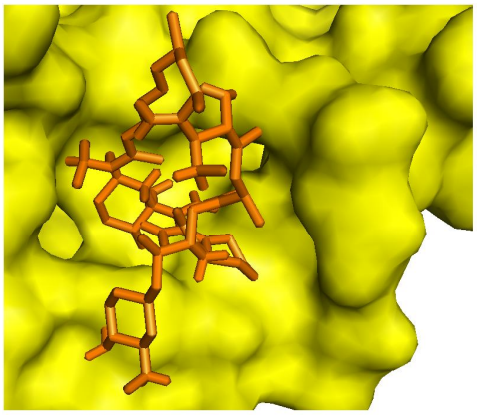

A. Binding pose of C. trachomatis (Y213A) with rapamycin

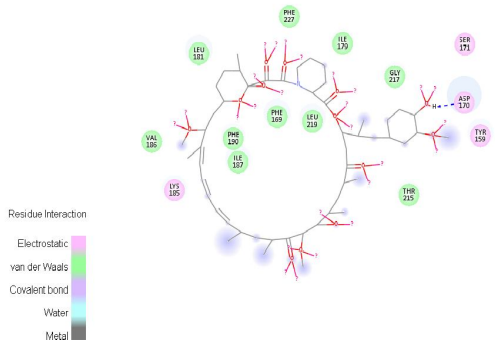

B. Hydrogen bond interactions for C. trachomatis (mutant) Y213A with rapamycin

Figure 6: Docking confirmation and hydrogen bonding interactions of *C. trachomatis* mutant (Y213A) with Rapamycin(A and B).

CONCLUSION:

The mutation D170L and Y213A was constructed in the putative active site region of *C. trachomatis* Mip played a major role to block the PPIase activity. The prediction of protein structural stability of the mutants (D170L) and (Y213A) were observed the loss of stability and probably

damaging by the I-Mutant 2.0 server. Docking experiment revealed that native Y213A Mip has the highest gold score of 37.17 in terms of rapamycin binding compared to D170L mutant has the 34.52 and and Y213A has 30.13 which indicates that the binding affinity is highly affected in the both the mutants due to structural changes in the active site due to mutagenesis thereby inhibiting the PPIase activity.. This study provides the importance of mutation study and will be very useful for the development of novel Mip inhibitors.

ACKNOWLEDGEMENTS:

The authors would like to thank Dr. Naidu Subbarao, Centre for Computational Biology and Bioinformatics, School of Computational and Integrative Sciences, Jawaharlal Nehru University, New Delhi, India for providing the Docking software for this work.

REFERENCES:

1. Chlamydia, Edited by Mihai Mares, 2012, Published by InTech Janeza Trdine 9, 51000 Rijeka, Croatia.
2. Wolf, K., Betts, H. J., Chellas-Géry, B., Hower, S., Linton, C. N. and Fields, K. A. (2006). Treatment of *Chlamydia trachomatis* with a small molecule inhibitor of the *Yersinia* type III secretion system disrupts progression of the chlamydial developmental cycle. Mol Microbiol. 61, 1543–1555.
3. Grayston J. T., Aldous, M. B., Easton, A, Wang, S.P., Kuo, C.C., Campbell, L.A. and Altman, J. (1993). Evidence that Chlamydia pneumoniae causes pneumonia and bronchitis. J Infect Dis. 168,1231-1235.
4. Mabey, D. C., A. W. Solomon, and A. Foster. (2003). Trachoma. *Lancet* 362, 223–229.
5. Lundemose, A. G., S. Birkelund, P. M. Larsen, S. J. Fey. and Christiansen. G. (1990). Characterization and identification of early proteins in *Chlamydia trachomatis* serovar L2 by two-dimensional gel electrophoresis. Infect. Immun. 58, 2478–2486.
6. Lundemose, A. G., Kay, J. E. and Pearce, J. H. **(**1993). *Chlamydia trachomatis* Mip-like protein has peptidyl-prolyl *cis*/*trans* isomerase activity that is inhibited by FK506 and rapamycin and is implicated in initiation of chlamydial infection. Mol. Microbiol. **7,** 777–783.
7. Riboldi-Tunnicliffe, A., Konig, B., Jessen, S., Weiss, M. S., Rahfeld, J., Hacker, J., Fischer, G., Hilgenfeld, R. (2001). Crystal structure of MIP, a prolylisomerase from Legionella pneumophila. Nature Struct Biol 8, 779–783.
8. Pedro José, B. P., Cristina Vega, M., Elena G. R., Rafael F. C., Sandra M. R., Gomis-Rüth, F.X., Antonio, G. and Miquel, C. (2002). *Trypanosoma cruzi* macrophage infectivity potentiator has a rotamase core and a highly exposed α-helix EMBO Rep. 3, 88–94.
9. Kissinger, C. R., Parge, H. E., Knighton, D.R., Lewis, C.T., Pelletier, L.A., Tempczyk, A., Kalish, V.J., Tucker, K.D., Showalter, R.E., Moomaw, E.W., et al. (1995). Crystal structures of human calcineurin and the human FKBP12-FK506-calcineurin complex. Nature. 7, 641-644.
10. Fischer, G., Bang, H., Ludwig, B., Mann, K, Hacker. J. (1992). Mip protein of *Legionella pneumophila* exhibits peptidyl-prolyl *cis/trans* isomerase (PPIase) activity. Mol Microbiol 6, 1375–1383.
11. Guba, M., Breitenbuch, V.P.,

Steinbauer, M., Koehl, G., Flegel, S., Hornung, M., Bruns, C.J., Zuelke, C., Farkas, S., Anthuber, M., Jauch, K.W., Geissler, E.K. (2002). Rapamycin inhibits primary and metastatic tumor growth by antiangiogenesis: involvement of vascular endothelial growth factor. Nature Med 8, 128–135.

12. Huai, Q., Kim, H.Y., Liu, Y., Zhao, Y., Mondragon, A., Liu, J.O. and Ke, H. (2002). Crystal structure of calcineurin- cyclophilin-cyclosporin shows common but distinct recognition of immunophilin- drug complexes. Proc Natl Acad Sci USA 99, 12037–12042.
13. Ke, H., Huai, Q. (2003). Structures of calcineurin and its complexes with immunophilins-immunosuppressants. Biochem Biophys Res Commun 311, 1095–1102.
14. Sharma, V.K., Li, B., Khanna, A., Sehajpal, P.K. and Suthanthiran, M. (1994). Which way for drug-mediated immunosuppression. Curr Opin Immunol 6, 784–790.
15. Wintermeyer, E., Ludwig, B., Steinert, M., Schmidt, B., Fischer, G. and Hacker, J. (1995). Influence of site specifically altered MIP proteins on intracellular survival of Legionella pneumophila in eucaryotic cells. Infect Immun 63, 4576–4583.
16. Vijayan, R., Subbarao, N. and Mallick, B. N. (2007). *In silico* modeling of α-1 A Adrenoceptor: Interactions of its Normal and Mutated Active sites with Noradrenaline as well as its Agonist and Antagonist. Am J Biochem Biotech. 3, 216-224.
17. McWilliam, H., Li, W., Uludag, M., Squizzato, S., Park, Y. M., Buso, N., Cowley, A. P. and Lopez, R. (2013). *Analysis Tool Web Services from the EMBL-EBI 2013*, Nucleic acids research 41(Web Server issue):W597-600.
18. Eswar, N., John, B., Mirkovic, N., Fiser, A., Ilyin, V. A., Pieper, U., Stuart, A. C., Marti-Renom, M. A., Madhusudhan, M. S., Yerkovich, B. and Sali, A. (2003). Tools for comparative protein structure modeling and analysis. Nucleic Acids Res. 31, 3375-3380.
19. Brooks, B. R., Bruccoleri, R. E., Olafson, B. D., States, D. J., Swaminathan, S. and Karplus, M. (1983). "CHARMM: A program for macromolecular energy, minimization, and dynamics calculations". *J Comp Chem* 4, 187–217.
20. Laskowski, R. A., MacArthur, M. W., Moss, D. S. and Thornton, J. M. (1993). PROCHECK: a program to check the stereochemical quality of protein structures. *J. Appl. Cryst.*, 26, 283-291.
21. Guex, N., Diemand, A. and Peitsch, M. C. (1999). Protein modelling for all. TiBS 24:364- 67.
22. Capriotti, E., Fariselli, P. and Casadio, R. (2005).I-Mutant2.0: predicting stability changes upon mutation from the protein sequence or structure. Nucl Acids Research 33, W306-W310.
23. Fraczkiewicz, R. and Braun, W. (1998). Exact and Efficient Analytical Calculation of the Accessible Surface Areas and Their Gradients for Macromolecules. *J. Comp. Chem.*, 19, 319-333.
24. The PyMOL Molecular Graphics System, Version 1.5.0.4 SchrÄodinger, LLC.
25. Huang, B. and Schroeder, M. (2006). LIGSITE*csc*: predicting ligand binding sites using the Connolly Surface and degree of conservation. BMC Structural Biology 6, 19.
26. Dundas, J., Ouyang, Z., Tseng, J., Binkowski, A., Turpaz, Y. and Liang, J. (2006). CASTp: computed atlas of surface topography of proteins with structural and topographical mapping

of functionally annotated residues. Nucleic Acids Research 34, 116-118.
27. Boyle N.M.O., James, B.M., Morley, C A., Vandermeersch, T. and Hutchison, G.R. (2011). Open Babel: An open chemical toolbox, Journal of Cheminformatics 3, 33.
28. Jones, G., Willett, P., Glen, R.C., Leach, A.R. and Taylor, R. (1997). Development and Validation of a Genetic Algorithm for Flexible Docking. Journal of Molecular Biology 267, 727-748.
29. Accelrys Software Inc., Discovery Studio Modeling Environment, Release 4.0, San Diego: Accelrys Software Inc., 2013.